Electronic Properties of Nitrogen-Doped Graphite Flakes

Dong-Pyo Kim,† C. L. Lin,† T. Mihalisin,† P. Heiney,‡ and M. M. Labes*,†

Departments of Chemistry and Physics, Temple University, Philadelphia, Pennsylvania 19122, and Department of Physics, University of Pennsylvania, Philadelphia, Pennsylvania 19104

Received February 22, 1991. Revised Manuscript Received May 23, 1991

Thermolyses of several nitrogen-containing heteroaromatic compounds were carried out at 800 °C, utilizing the identical experimental conditions under which benzene forms graphite flakes, to yield nitrogen-doped graphitic flakes (NDGs) having similar disordered structures. Heat treatment of the NDGs in the range 1000–1600 °C results in an increase of the graphitic order with some retention of significant nitrogen content (between 0.5 and 6.4%). These NDGs show low-temperature electronic behavior strikingly different from the benzene-derived carbons: (a) a strong decrease in low-temperature resistivity (ρ) with decreasing temperature and (b) negative magnetoresistance at low magnetic fields applied parallel to the c axis. In these ways NDGs resemble doped semiconductors in their electronic properties, whereas the pure benzene-derived carbons can best be treated in terms of a variable-range hopping mechanism.

Introduction

Conceptually, the introduction of either boron or nitrogen into a graphite lattice should significantly modulate its band structure.[1] In terms of size, both atoms are not too unlike carbon, and boron is known with certainty to enter substitutionally into the trigonal lattice sites of graphite and function as an acceptor dopant.[2] Incorporation of nitrogen into carbons has been attempted by the thermal decomposition of appropriate precursors,[3] the most widely studied material being poly(acrylonitrile) (PAN), which can be spun into fibers and then heat treated to yield carbon fibers. In the final stages of carbonization of PAN,[4] nitrogen is believed to be eliminated as molecular nitrogen. The model that has been suggested involves the formation of graphite domains with nitrogen and hydrogen migrating to the periphery of these domains.[5] Finally at higher temperatures, domains are thought to consolidate with the elimination of nitrogen and hydrogen. In studies of the thermal decomposition of poly(oxadiazole), followed via photoelectron spectroscopy, Murakami et al. claimed incorporation of nitrogen into lattice sites starting at 800 °C, but the technique was not sufficiently sensitive to follow the higher temperature processes.[6]

In our recent work,[7] we have established a new method of preparing graphitic materials in flake form. Various precursors such as benzene or triphenylene, as examples of condensed ring aromatic hydrocarbons, can produce flakes in relatively large quantities (~50 g of product in a tube furnace) with reproducible morphological, electronic, and mechanical properties. What differs in the microstructure as a function of precursor is the degree and nature of residual disorder after various temperature anneals; at the highest heat treatment temperatures (2600 °C) the materials approach single-crystal graphite in their properties. As a consequence of this common morphology, this method of preparation allows us to prepare doped graphites from heteroaromatic precursors that can be directly compared to the pure carbon samples. In this paper, we describe nitrogen-doped graphites (NDGs) prepared in this manner.

The interpretation of the electronic properties of disordered conductors has followed two approaches: The first starts with a classical two-dimensional band structure in which one introduces a distribution of localized states caused by impurities or defects across the bandgap. The main effect of doping such a solid is a lowering or raising of the Fermi level upon the addition of acceptors or donors, respectively.[2] If such a model applies, one would expect resistivity to increase with decreasing temperature at low temperatures. In the more ordered graphites, such as single-crystal graphite, pyrolytic graphite, and benzene-derived fibers annealed over 3000 °C, there is a decrease of basal plane resistivity with temperature in the range 20–60 K.[8]

The second interpretation analyzes the anomalous transport properties of electrons in disordered systems by considering single-electron motion, weak localization, electron–electron interactions, and Coulomb interactions. To understand the electronic properties and attempt distinctions between these approaches, resistance anomalies at low temperature and magnetoresistance (MR) have been intensively studied.[9] In this work, such a study is undertaken on NDGs and, for comparison purposes, on disordered carbons prepared from benzene (B).

In both the cases where nitrogen exists at substitutional lattice sites or at the periphery of a domain, one might expect to affect the electronic properties of these intermediate carbons. For this reason it is interesting to explore the preparation and properties of NDGs in some detail. If one finds evidence for significant modulation of the electronic properties, attempts to stabilize such lattices at high temperatures and pressures would appear worthwhile. In this context it is interesting to note that nitrogen incorporation into diamond introduces color, decreases thermal conductivity, and increases hardness.[10]

Experimental Section

Benzene (B), pyrazine (PZ), pyridine (PR), quinoline (QN),

†Temple University.
‡University of Pennsylvania.

(1) Kaner, R. B.; Kouvetakis, J.; Warble, C. E.; Sattler, M. L.; Bartlett, N. *Mater. Res. Bull.* **1987**, *22*, 399. Moore, A. W.; Strong, S. L.; Spain, I. L.; Dresselhaus, M. S.; Piraux, L. *J. Appl. Phys.* **1989**, *65*, 5109.
(2) Marchand, A. *Chemistry and Physics of Carbon*; Marcel Dekker: New York, 1971; Vol. 7, p 155.
(3) Chiang, L. Y.; Stokes, J. P.; Johnston, D. C.; Goshorn, D. P. *Synth. Met.* **1989**, *29*, E483. Kouvetakis, J.; Kaner, R. B.; Sattler, M. L.; Bartlett, N. *J. Chem. Soc., Chem. Commun.* **1986**, 1758.
(4) Donnet, J. B.; Bansal, R. C. *Comprehensive Polymer Science*; Pergamon Press: Oxford, 1989; Vol. 7, p 501.
(5) Murakami, M.; Yoshimura, S. *Synth. Met.* **1987**, *18*, 509.
(6) Murakami, M.; Yasujima, H.; Yumoto, Y.; Mizogami, S.; Yoshimura, S. *Solid State Commun.* **1983**, *45*, 1085.
(7) Kim, D.; Labes, M. M. *Chem. Mater.* **1990**, *2*, 599.
(8) Kulbachinskii, V. A. *Phys. Status Solidi B* **1989**, *151*, 185. Woolf, L. C.; Chin, J.; Lin-Liu, Y. R.; Ikezi, H. *Phys. Rev. B* **1984**, *30*, 861.
(9) Rosenbaum, T. F.; Milligan, R. F.; Paalanen, M. A.; Thomas, G. A.; Bhatt, R. N.; Lin, W. *Phys. Rev. B.* **1983**, *27*, 7509. Ootuka, Y.; Kabayasi, S.; Ikehata, S.; Sasaki, W. *Solid State Commun.* **1979**, *30*, 169.
(10) Bachmann, P. K.; Messier, R. *Chem. Eng. News* **1989**, *67*(20), 24. Burgemeister, E. A. *Physica* **1978**, *93*, 165.

0897-4756/91/2803-0686$02.50/0

and phenazine (PN) were obtained from Aldrich Chemical or Eastman Kodak and employed without purification. Carbonizations were carried out in a tube furnace at 800 °C as previously described.[7] The liquid starting materials B, PR, and QN were purged into the hot zone of a quartz tube by bubbling argon carrier gas into the liquid contained in a flask heated at 50, 80, and 200 °C, respectively. Solid PN and PZ were placed in an inlet adaptor heated to about 250 and 90 °C, respectively. These conditions provided essentially the same vapor pressure of each starting material of about 300 mmHg.

All the materials yielded well-formed flakes, which were subsequently graphitized in a high-temperature furnace (Thermal Technology Group 1000) that was fitted with a graphite hearth. The samples were placed in a graphite crucible and heated under high-purity grade helium for periods of 1 h at a heat treatment temperature (HTT) of 900–2600 °C. The heating processes were controlled by a digital control programmer (Honeywell DCP 700) as follows: 1 h of linear heating to 1200 °C, followed by 0.5-h anneal at that temperature, followed by heating at rates of 800 and 600 °C/h to 2000 and 2600 °C, respectively. Elemental analyses were conducted to determine the content of nitrogen in the samples by Huffman Laboratory.

X-ray diffraction (XRD) data were obtained on a Rigaku D/Max2 instrument, using Cu Kα radiation. Film samples were attached to Kapton 3M no. 92 tape for XRD. Additional XRD determinations to measure the mosaic spread using Mo Kα radiation were performed at the University of Pennsylvania.

The thickness (5–40 μm), length (5–10 mm), and width (1–2 mm) of the samples were measured with a digital micrometer and optical microscope, respectively. Photomicrographs of the surface morphology of the samples were taken by using scanning electron microscopy (SEM). To perform MR measurements, 0.05-mm platinum wires and no. 40 copper wires were attached by using silver conducting adhesive to a five-sample series mounted on a sapphire block. Up to 10 samples (mounted on two sides of an aluminum sample block) could be measured simultaneously to determine the zero-field ρ and the MR with I (current) $\perp$ H (magnetic field) $\perp$ c axis of graphite. MR could also be measured in another sample arrangement, I (current) $\perp$ H (magnetic field) $\parallel$ c axis of graphite, by attaching the same samples on a sapphire substrate to the bottom of the same aluminum block. The vacuum can containing the sample block was sealed by using an indium O-ring, evacuated to 1×10^{-6} Torr, and leak checked. The probe rod was then placed in a Dewar assembly.

The ρ of each sample was measured from 0.5 to 300 K in magnetic fields up to 40 kG (4 T) by using a standard four-probe dc technique. An automatic data acquisition system, which was controlled by an HP9816 microcomputer interfaced with Keithley measuring devices, was used to take the measurements. Two Keithley constant-current sources (K220) with the capability of reversing the current direction were used to provide a current of 1–10 μA to the samples and thermometer dc current. The output voltage from a Keithley power supply (K230) was used to power the heater. A Keithley nanovoltmeter (K181) was used to measure sample voltage, and a Keithley voltmeter (K193) was used to measure the thermometer voltage. By use of a low-noise Keithley scanner (K705), it was possible to collect data on several samples during the same run.

After the computer started to acquire data at room temperature, the outer Dewar was filled with liquid nitrogen, and the probe cooled down slowly to 80 K overnight. Liquid helium was then transferred slowly to the inner glass Dewar to lower temperatures of 10 K. When the sample block cooled down below 10 K, a needle valve was opened and the inner He^4 pot allowed to fill. After the He^4 pot was pumped, the temperature of the sample block dropped to about 1.5 K within 10 min. He^3 gas was then introduced into the probe through the He^3 pumping line. Pumping on the liquid He^3 that condensed in the He^3 pot allowed the temperature of the sample block to drop to about 0.5 K. The heater and drift mode of the computer ρ program made it possible to measure data under reliable conditions.

To determine the MR, a superconducting magnet was mounted over the vacuum can and provided magnetic fields up to 40 kG. Temperature was read by two thermometers, Ge (germanium) and CG (carbon glass) resistor, which were calibrated in the temperature ranges 0.4–5 and 1.2–300 K, respectively. The temperature of the samples glued to the aluminum sample block was controlled by regulating the current to the heater. All the solder connections were made by using a cadmium/tin low-noise solder to minimize thermally induced emf's.

A Bruker ER200D-SRC electron spin resonance spectrometer (ESR) was used to measure the spin density of powder samples at 300 K. Spin concentration was determined by comparing the intensity of the sample with that of a reference substance, diphenylpicrylhydrazyl (DPPH).

Table I. Dependence of Lattice d Spacing, Crystallite Size along c Axis (L_c), and Mosaic Spread on Heat Treatment Temperature for Benzene-Derived Graphites and NDGs

sample[a]	d spacing, Å	L_c, Å	mosaic spread, deg
B1500	3.44	53	
B2000	3.42	154	4
B2300	3.38	258	
B2600	3.36	351	8
NDG1200	3.43	42	27
NDG1600	3.44	65	25
NDG2000	3.42	152	21
NDG2300	3.38	242	18
NDG2600	3.36	335	17

[a] Numbers indicate heat treatment temperature. Values of NDGs are the average of PR-, QN-, PN-, and PZ-derived graphites.

Table II. Elemental Analyses and Nitrogen Content in NDGs at Different HTTs

		HTT, %			
sample	initial %N	800 °C	1000 °C	1200 °C	1600 °C
PZ	36.8	5.4		2.0	0.5
PR	18.9	6.1	5.9	1.2	
QN	11.5	4.5		0.8	
PN	16.3	8.6	6.4	2.4	

Results and Discussion

Table I presents structural information on B-derived graphites and NDGs. Virtually no XRD is observed below a HTT of 1000 °C. At HTTs of 1200 and 1600 °C, the XRD consists of only broad, weak (002) lines, indicating that the samples are at an early stage of graphitization and that the basal plane of the developing graphite lattice is parallel to the surface of the flakes. Above HTTs of 2000 °C, d spacing and layer thickness are determined from the (004) line. In both B-derived graphites and NDGs, the d spacing reaches graphite-like values at essentially the same rate, proceeding from a poorly oriented state with a d spacing of 3.44 Å to an oriented state with a d spacing of 3.36 Å.[7] At the same time L_c increases to about 350 Å in both sets of samples.

There is, however, a considerable difference in the extent of orientation of the polycrystalline domains—the "mosaic spread", defined as the full width at half-maximum intensity of the (002) line obtained from an intensity scan versus θ (incident angle) at fixed 2θ (diffracted angle). For NDGs, the mosaic spread is wider than that of B-derived graphites. This effect appears to be due to a puffing phenomena associated with the elimination of nitrogen from the structure,[11] followed by orientation between domains at the higher HTTs. An example of this puffing effect can be seen in Figure 1.

It is known that nitrogen is eliminated out of a carbon structure at high temperatures and that the matrix undergoes growth and orientation of graphitic domains. Table II shows the dependence of the nitrogen content on HTT and the nature of the heteroaromatic precursor. In

(11) Fujimoto, K.; Mochida, I.; Todo, Y.; Oyama, T.; Yamashita, R.; Marsh, H. *Carbon* **1989**, *27*, 909.

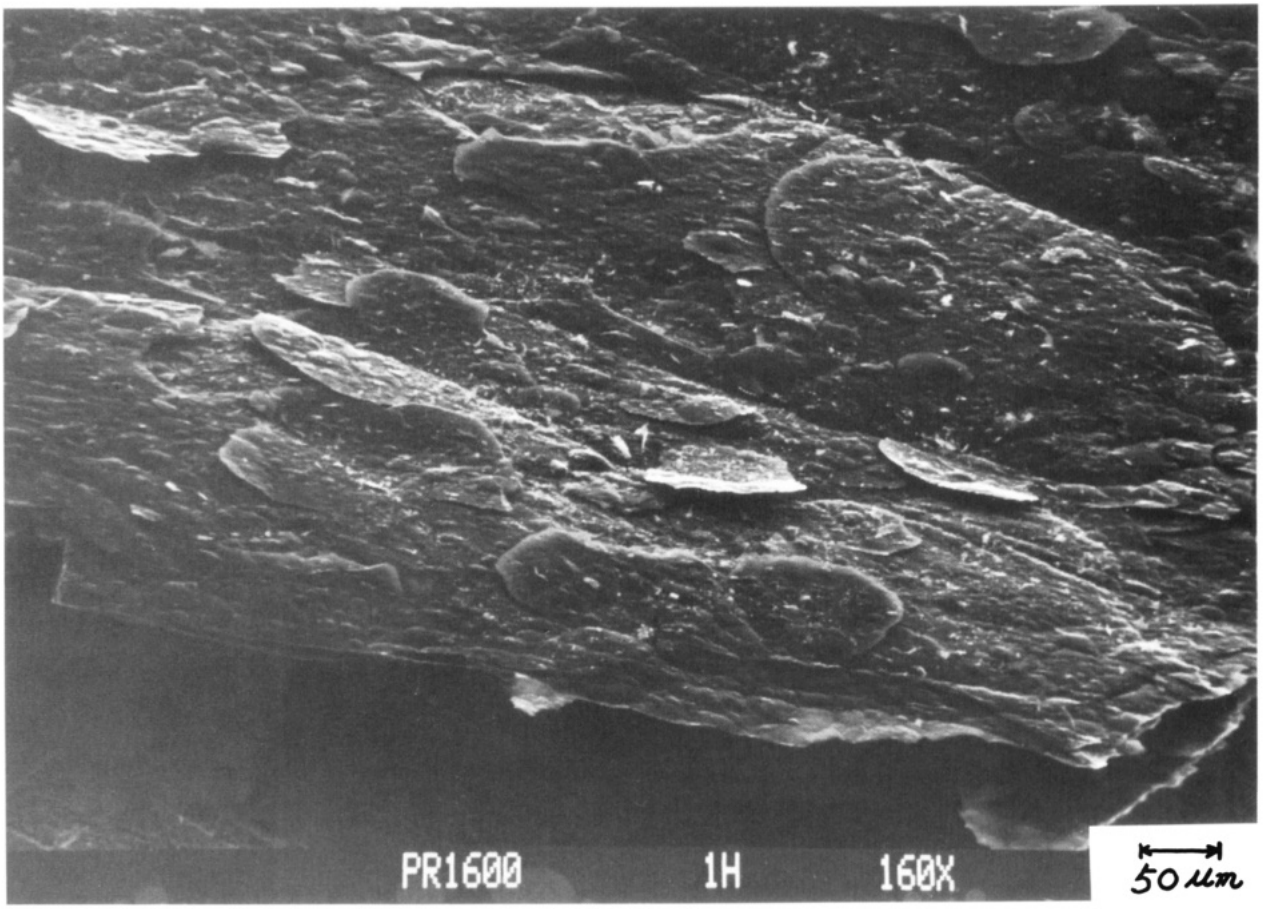

Figure 1. Scanning electron microscopic view of PR1600 flake. PR = pyridine. Number indicates HTT in °C.

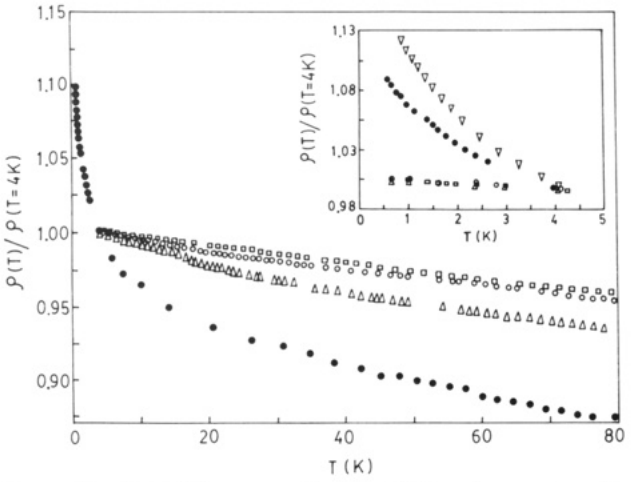

Figure 2. Resistivity normalized to 4 K vs temperature for B-derived carbons. B800, ▽; B900, ●; B1200, □; B1600, ○; B2000, △. B = benzene, number indicates HTT in °C.

the initial 800 °C processing, chlorine is used as a catalyst,[12] but no chlorine is found in these materials within the analytical limits. Nitrogen contents vary strongly with precursor in the carbons formed at 800 °C. Less than 2.4% is found in the NDGs after heating to 1200 °C for 1 h. In PAN-derived carbon fibers, it is reported that all nitrogen is eliminated at about 1700 °C.[4] In the PZ-derived carbon flake, 0.5% nitrogen persists at 1600 °C.

Dependence of ρ on T at Zero Magnetic Field. In B-derived carbons, the dependence of ρ on temperature is a strong function of the HTT (Figure 2). Samples heat

Table III. Resistivity and Resistance Ratio $\rho_{4.2K}/\rho_{293K}$ for Pure Carbons and NDGs

sample	HTT, °C	resistivity, S cm^{-1} 293 K	resistivity, S cm^{-1} 4.2 K	ratio $\rho_{4.2K}/\rho_{293K}$
PZ	1200	1.86×10^{-3}	2.21×10^{-3}	1.19
PR	900	2.42×10^{-3}	2.85×10^{-3}	1.18
PR	1200	2.69×10^{-3}	2.98×10^{-3}	1.11
PR	1600	2.32×10^{-3}	2.65×10^{-3}	1.14
PR	2000	2.51×10^{-4}	5.96×10^{-4}	2.37
QN	1200	1.40×10^{-3}	1.66×10^{-3}	1.19
QN	1600	2.00×10^{-3}	4.22×10^{-3}	2.11
QN	2000	3.98×10^{-4}	1.02×10^{-3}	2.56
PN	1200	8.07×10^{-3}	1.02×10^{-2}	1.26
PN	1600	2.17×10^{-3}	2.52×10^{-3}	1.16
PN	2000	1.64×10^{-4}	3.84×10^{-4}	2.34
B	800	3.17×10^{-3}	5.03×10^{-3}	1.59
B	900	2.51×10^{-3}	3.72×10^{-3}	1.48
B	1200	1.01×10^{-3}	1.15×10^{-3}	1.14
B	1600	7.30×10^{-4}	8.45×10^{-4}	1.16
B	2000	3.29×10^{-4}	4.09×10^{-4}	1.24

treated at 800 and 900 °C show a marked increase in ρ with decreasing temperature, whereas samples heat treated at 1200 °C and above exhibit a relatively constant ρ below 4 K. Note that the high-temperature slopes of these lines become greater at higher HTT, which implies a decrease in the population of localized states causing an expansion of the band gap (Table III). Below 1000 °C, it appears reasonable to interpret ρ as being governed by a variable-range hopping mechanism.[6,13] For such a transport process, one typically finds ln ρ to depend on $1/T$ at ordinary temperatures (Figure 3). The activation energy

(12) Stacy, W. O.; Walker, P. L. *Carbon* **1966**, *4*, 343.

(13) Miyake, K.; Shimakawa, K. *Phys. Rev. B* **1989**, *39*, 7578. Hishiyama, Y.; Kaburagi, Y.; Ono, A. *Carbon* **1979**, *17*, 265.

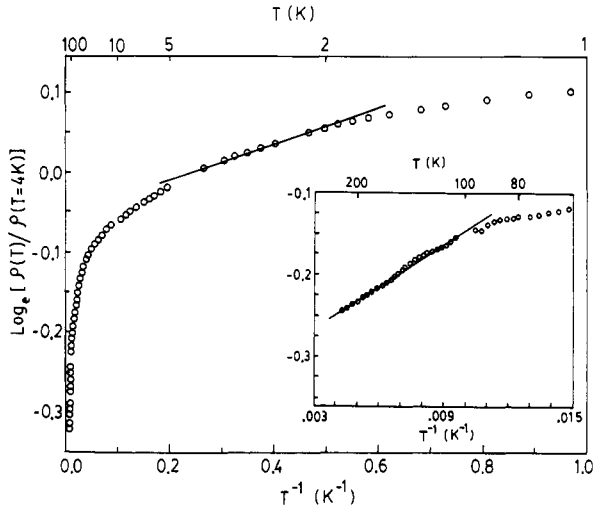

Figure 3. ln resistivity normalized to 4 K vs reciprocal T for B800.

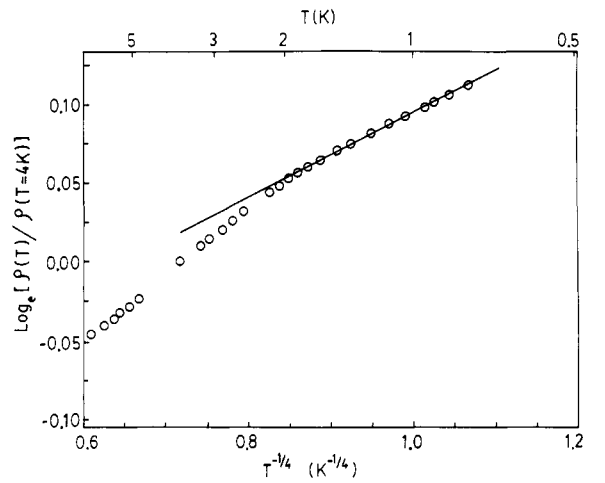

Figure 4. ln resistivity normalized to 4 K plotted as a function of $T^{-1/4}$ for B800.

in fact decreases gradually with decreasing temperature, suggesting that (at least) two transport mechanisms are involved: thermal activation to the mobility edge at higher temperatures, and variable-range hopping at lower temperatures, ultimately showing the dependence ln ρ vs $T^{-1/4}$. This dependence is most clearly shown in the as-deposited carbon at 800 °C when one measures ρ below 2 K (Figure 4).

The dependence of ρ on T for the NDGs is quite different from that of B (Figure 5). ρ shows a maximum at about 30 K, and a metallic temperature dependence below this, finally levelling off at very low temperatures. These differences are most likely due to the presence of traces of the donor atom N in the carbons. The samples behave similarly to small-bandgap semiconductors[9] or metallomacrocycles[14] doped to a level above some critical concentration of donors. In such cases, the decrease in the low-temperature ρ has been interpreted as being largely due to Coulomb interactions.[9,15] Such materials are expected to be quite sensitive to dopant level, which is, of course, varying quite markedly as a function of HTT in the NDGs. In these doped carbons it is also quite likely that the bandgap is varied by the donor level. The extent of disorder in the samples also varies with HTT, making a detailed interpretation rather complicated.

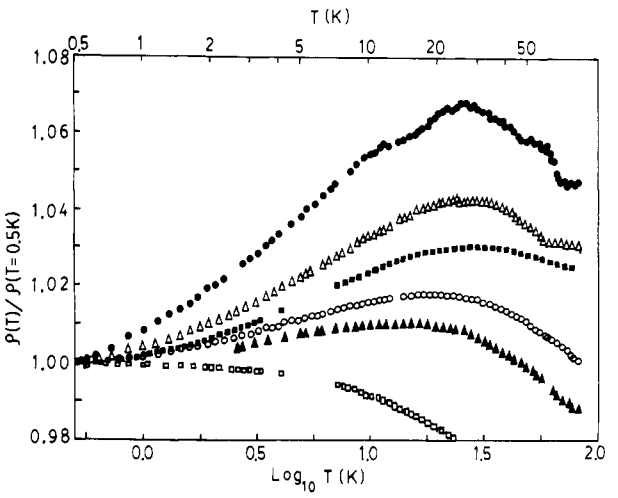

Figure 5. Resistivity normalized to 0.5 K of nitrogen-doped graphites (NDGs) vs log T at different HTTs. PR900, ●; PZ1200, △; QN1200, ■; PR1600 (annealed for 10 min), ○; PN1600, ▲; QN2000, □. PR = pyridine, PZ = pyrazine, QN = quinoline, PN = phenazine.

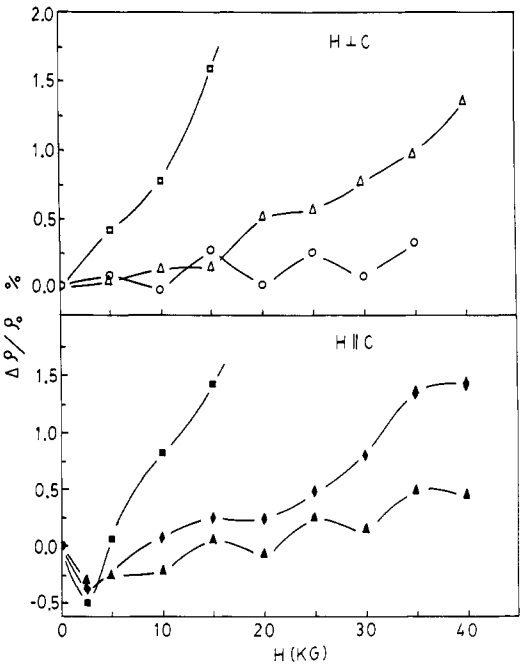

Figure 6. MR of PR900 at various applied magnetic fields H. Upper curves: $H \perp c$ axis; ○, 10 K; △, 4 K; □, 1 K. Lower curves: $H \parallel c$ axis; ▲, 4 K; ◆, 2.5 K; ■, 1 K. PR = pyridine.

In contrast to what one finds in doped semiconductors, Table III illustrates that the resistivities of NDGs are of the same order of magnitude as those of B-derived carbons at each HTT. It is well-known that crystalline semiconductors are extremely sensitive to doping with an impurity element because of the ultralow density of states in the bandgaps of these materials. However, the situation is not as straightforward in amorphous semiconductors because the density of states function is continuous throughout the band.[16] The insensitivity of the resistivity of NDGs to doping level may be ascribed to a mixed-band structure of localized states at and above the Fermi level, arising from the highly disordered structure of pyrolytic carbons, and donor levels. In such a situation, free propagation of conduction electrons is limited by the high defect density.

(14) Marks, T. J. *Angew. Chem., Int. Ed. Engl.* **1990**, *29*, 857.
(15) Bergmann, G. *Phys. Rev. B* **1987**, *35*, 4205. Lee, P. A.; Ramakrishnan, T. V. *Rev. Mod. Phys.* **1985**, *57*, 287.

(16) Jonscher, A. K.; Hill, R. M. *Physics of Thin Films*; Academic Press: New York, 1975; Vol. 8, p 170.

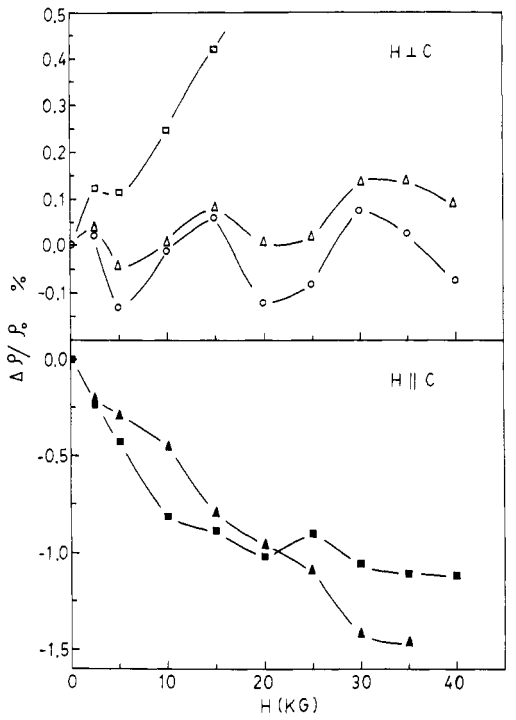

Figure 7. MR of PR1600 at various applied magnetic fields H. Upper curves: $H \perp c$ axis; ○, 10 K; △, 4 K; □, 1 K. Lower curves: $H \parallel c$ axis; ▲, 4 K; ■, 1 K. PR = pyridine.

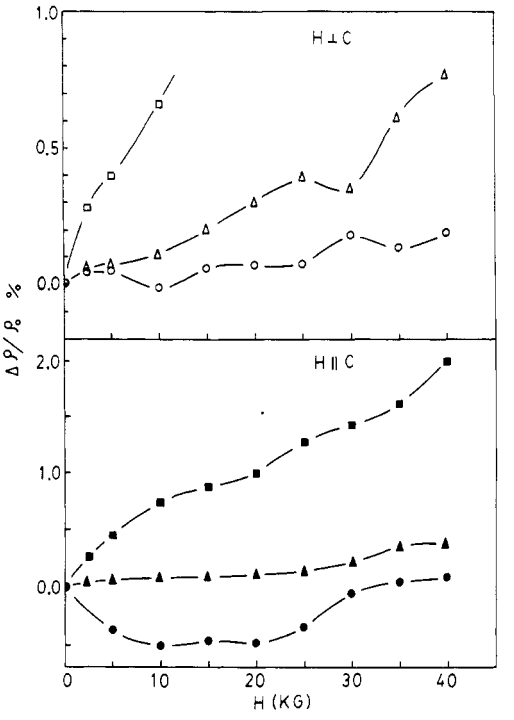

Figure 8. MR of B800 at various applied magnetic fields H. Upper curves: $H \perp c$ axis; ○, 10 K; △, 4 K; □, 1 K. Lower curves: $H \parallel c$ axis; ●, 10 K; ▲, 4 K; ■, 1 K. B = benzene.

Dependence of MR on HTT, H, and T. In NDGs heat-treated to temperatures below 1000 °C, the MR increases with increasing H and with decreasing T, and there is essentially no anisotropy of the MR with direction of the applied H (Figure 6). As HTT is increased to 1600 °C, however, there is a marked difference in the MR between $H \perp c$ axis and $H \parallel c$ axis (Figure 7). Indeed, one would expect the case of $H \parallel c$ axis to be more structure sensitive than the case $H \perp c$ axis, since the motion of carriers by Lorentz forces is confined primarily to the basal plane. For $H \perp c$ axis, the MR at 1 K is positive over the entire range of applied fields studied, while for $H \parallel c$ axis MR changes from positive to negative as one approaches an HTT of 1600 °C. The development of a turbostratic form of graphite from a disordered structure is most likely responsible for this anisotropy.[17] At an HTT of 1200 °C, the MR first begins to show a weakly anisotropic dependence on the direction of H, while at an HTT of 900 °C the behavior is isotropic.

In the view that it is reasonable to treat an NDG as mechanistically similar to a doped narrow-bandgap semiconductor, one would expect a positive MR to arise from Coulomb interactions, and a negative MR to be due to localization effects in the disordered structures.[9] For NDGs at HTTs of 1200 and 1600 °C, the MR with $H \parallel c$ axis tends to saturate at high fields and high ambient temperature, while the absolute magnitude of the negative MR increases at low field (Figure 7). The behavior implies some superposition of factors leading to positive and negative MRs. Especially for NDGs annealed at 900 °C with $H \parallel c$ axis, at low fields Coulomb interactions would be expected to be hardly perturbed, and therefore field-sensitive localization effects would dominate to produce a negative MR while B-derived carbon deposited at 800 °C shows a positive MR through all fields range (Figure 8). Although the resistivity-temperature dependencies of

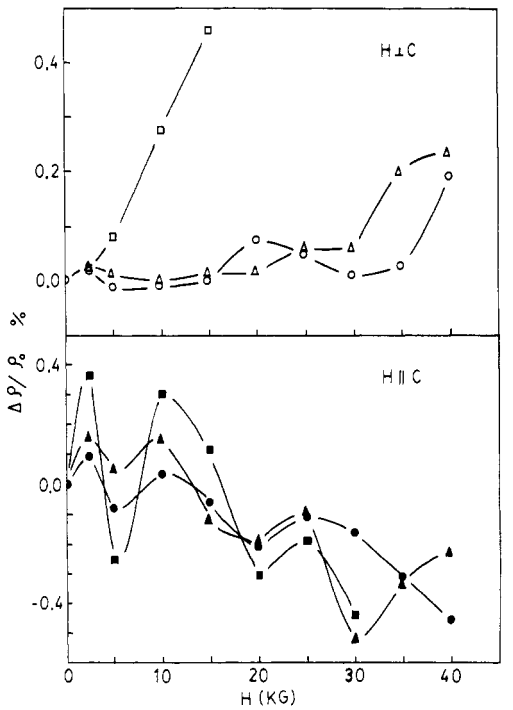

Figure 9. MR of B1200 at various applied magnetic fields H. Upper curves: $H \perp c$ axis; ○, 10 K; △, 4 K; □, 1 K. Lower curves: $H \parallel c$ axis; ●, 10 K; ▲, 4 K; ■, 1 K. B = benzene.

the NDGs are similar to those of well-oriented pyrolytic graphites, the negative MR of NDGs at low fields indicates their electronic origin must be different from the positive MR of well-oriented pyrolytic graphites.

Over 1600 °C, when nitrogen is virtually eliminated from the sample, the magnetoresistive behavior is essentially identical with that of B-derived carbons, in which negative MR is found at all applied H's (Figure 10). The MR becomes negative when the disordered carbon structure transforms to a turbostratic structure with increasing

(17) Delhaes, P. *Chemistry and Physics of Carbon*; Marcel Dekker: New York, 1971; Vol. 7, p 193.

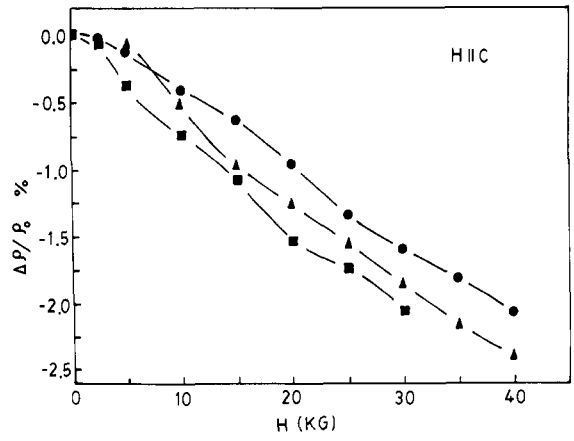

Figure 10. MR of B1600 at various applied magnetic fields H. $H \parallel c$ axis; ●, 10 K; ▲, 4 K; ■, 1 K. B = benzene.

HTT. For HTTs of 1600 and 2000 °C, the absolute magnitude of the negative MR increases with increasing H field and decreasing T. This type of behavior above an HTT of 2000 °C was recently interpreted as resulting from the sum of two contributions: a weak localization effect, which gives rise to an extra resistivity at low temperature, and the classical Boltzmann contribution, which involves the temperature dependence of both the mobility and carrier density.[18] The magnitude of the weak localization contribution decreases as the degree of graphitization increases, and eventually the slope of the low-temperature resistivity is reversed from negative to positive around 30 K. This result provides strong support for the interpretation of the negative MR in pregraphitic materials in terms of weak localization.

Shubnikov–de Haas (SdH) Oscillatory MR. When an H field is applied, the magnetic energy levels become quantized (Landau levels), which may give rise to oscillation in the resistivity with changing H.[19] Since SdH oscillations are due to levels near the Fermi energy that almost always have high quantum numbers, they may give information about the electronic band structure that is entirely determined by the shape of the Fermi surface. Their measurement usually requires single crystals or large crystallite size and negligible boundary scattering at very low temperatures and is frequently performed in very strong H. Some measurements have been performed on less-than-ideal structures, for example, ordinary carbon fibers show no SdH oscillations, whereas highly ordered graphites having large crystallite size and $CuCl_2$-intercalated fibers exhibit SdH oscillation superimposed on a large positive MR at low T and high H.[20]

We report here some preliminary observations of similar oscillations when the materials are still significantly disordered (Table I and Figures 6 and 7), and the sign of the MR changes from positive to negative and then back to positive. Unusual oscillations are shown in the HTT range 900–1600 °C. In the B-derived graphites, they are seen at several HTTs but most clearly at 1200 °C (Figure 9). Strictly speaking the SdH terminology should be restricted to samples having a positive MR, but the oscillatory behavior noted here is most likely closely related.

Table IV. Comparison of ESR Spin Densities, g Values, and Line Widths of Pure Carbons and NDGs Heat Treated at 800 °C[a]

sample	HTT, °C	g	spin density, 10^{18} spins g^{-1}	line width, G
B	800	2.002 542	10	1.05
PZ	800	2.002 658	240	1.47
PR	800	2.002 677	150	1.20
QN	800	2.002 608	154	1.39
PN	800	2.003 899	216	1.59

[a] Measurements were conducted at 300 K.

At this point it should be noted that there have also been reports of unusual oscillations in pitch-derived fibers even under negative MR[21] and in organic conducting charge-transfer salts[22] and pyrolytic carbons deposited under a nitrogen atmosphere at 1800–1900 °C, which are probably doped at a very low level with nitrogen.[23]

Electron Spin Resonance (ESR) Measurements. In homogeneous semiconductors, the coexistence of localized spin centers and conduction carriers can be detected by ESR. Only one resonance line is observed because of the interaction between the two kinds of paramagnetic centers.[24] The random localized electrons with their magnetic moments influence the scattering of conduction electrons through exchange interaction.[15,25] Table IV presents a comparison of ESR data for B-derived carbons and NDGs. ESR spectra on the fine-particle samples showed a symmetric line shape, in other words, the *absence* of Dysonian behavior, indicating that the particle size is less than the skin depth at HTT of 800 °C. Further, no well-resolved peaks were observed, indicating that anisotropic orientation does not develop below an HTT of 1000 °C as indicated in the XRD. Samples annealed at higher HTTs show extreme line broadening with increasing HTT.[7] For an NDG at a HTT of 800 °C, the spin density is of the order 10^{20} spins g^{-1}, whereas the B-derived carbons contain 10^{18}–10^{19} spins g^{-1}. The ESR spectra of PZ-, PR-, and QN-derived NDGs are characterized by nearly free-electron g values and broader line widths than those for B-derived carbon, due to delocalized conduction electrons presumably arising from nitrogen doping.[26]

Concluding Remarks

There are large differences in the electronic properties of disordered carbons from a hydrocarbon source and a nitrogen-containing source that reflect themselves in the temperature dependences of the resistivity and the MR, as well as the H field dependence of the latter. In addition unusual oscillatory phenomena and ESR spectroscopic differences are evident in the NDGs. It is extremely difficult to fully understand these phenomena in detail because both disorder and doping perturb the electronic structure of the materials. Nevertheless, by comparison of the properties of the benzene-derived graphites to those of the NDGs, it seems likely that nitrogen doping does perturb the material in a significant way. Achieving order in these materials will require high-pressure and high-temperature annealing, and efforts in this regard are now underway.

(18) Bayot, V.; Piraux, L.; Michenaud, J.; Issi, J.; Lelaurain, M.; Moore, A. *Phys. Rev. B* **1990**, *41*, 11770. Bayot, V.; Piraux, L.; Michenaud, J.; Issi, J. *Phys. Rev. B* **1990**, *40*, 3514.
(19) Ashcroft, N. W.; Mermin, N. C. *Solid State Physics*; Saunders College: Philadelphia, 1976; p 264. Nakamura, M. J. *Phys. Soc. Jpn.* **1967**, *22*, 830.
(20) Natarajan, V.; Woollam, J. A.; Yavrouian, A. *Synth. Met.* **1983**, *8*, 291. Chieu, T. C.; Timp, G.; Dresselhaus, M. S.; Endo, M.; Moore, A. W. *Phys. Rev. B* **1983**, *27*, 3686.
(21) Woolf, L. D.; Ikezi, H.; Lin-Liu, Y. R. *Solid State Commun.* **1985**, *54*, 49.
(22) Azbel, M. Y.; Chaikin, P. M. *Phys. Rev. Lett.* **1987**, *59*, 582.
(23) Takeya, K.; Yazawa, K.; Okuyama, N.; Akutsu; Ezoe, F. *Phys. Rev. Lett.* **1965**, *15*, 110.
(24) Mrozowski, S. *Carbon* **1988**, *26*, 521.
(25) Fukase, T.; Koike, Y. *Solid State Commun.* **1987**, *62*, 499.
(26) Robson, D.; Assabghy, F. Y. Z.; Ingram, D. J. E. *J. Phys. D, Appl. Phys.* **1971**, *4*, 1426. Hasegawa, S.; Shimizu, T. *Jpn. J. Appl. Phys.* **1970**, *9*, 958.

Acknowledgment. We thank Dr. S. Jansen for helpful discussions regarding the ESR measurements. This work was supported in part by the National Science Foundation, Ceramics and Electronic Materials, Division of Materials Research, under Grant No. DMR87-03526. The XRD measurements at University of Pennsylvania were performed by using central facilities of the Laboratory for Research on the Structure of Matter, supported by the National Science Foundation Grant No. DMR MRL 88-19885.

Low-Temperature Syntheses of Olivine and Forsterite Facilitated by Hydrogen Peroxide

James M. Burlitch,* Mark L. Beeman,† Bart Riley,‡ and David L. Kohlstedt§

Departments of Chemistry and Materials Science and Engineering, Cornell University, Ithaca, New York 14853-1301

Received March 12, 1991. Revised Manuscript Received May 14, 1991

The use of an iron carbonyl, in combination with metal alkoxides, produced a new route to precursors for olivine ($(Mg_{0.9}Fe_{0.1})_2SiO_4$, Fo_{90}). The principal iron-containing intermediates, pentacarbonyliron and a low-valent, anionic metal carbonyl, produced by the reduction of $Fe_2(CO)_9$ by magnesium metal and $Mg(OMe)_2$ in the presence of $Si(OEt)_4$, were soluble in methanol. The iron-containing components were smoothly incorporated into the sol when the mixture of alkoxides was simultaneously hydrolyzed and condensed by the addition of aqueous hydrogen peroxide. H_2O_2 served at least two important functions: (1) it sequestered magnesium, thereby preventing precipitation of magnesium hydroxide; (2) it partially oxidized the iron carbonylate intermediates. After calcination, firing of pre-Fo_{90} powders at 1200–1300 °C in a CO/CO_2 atmosphere readily converted them to single-phase, crystalline olivine. Hot-pressing the resulting powder gave fine-grained, dense, solid specimens. DTA data and separate firings in an atmosphere of H_2 and CO_2 demonstrated that firing temperatures as low as 850 °C were sufficient to produce crystalline olivine. Without iron, synthetic forsterite, Mg_2SiO_4, was the sole product in a process that required no added strong acid or base as a catalyst for hydrolysis of $Si(OEt)_4$. Calcined forsterite precursor powders were converted to single-phase forsterite that was partially crystallized at 750 °C and fully crystalline at 1000 °C.

Introduction

The importance of magnesium and iron silicates predates recorded history; major components of the earth's upper mantle are aggregates or composites that contain these ceramic materials. Consequently, the study of their mechanical behavior is of considerable importance because many geological processes, involving movement of these materials, depend on their rheological properties.[1] Synthetic samples of such aggregates are needed for mechanical properties' measurements because (i) natural materials have uncontrollable amounts of various other components and (ii) fine-grained rocks, which are required to investigate deformation via diffusion mechanisms, are not available at the surface of the earth. Classical "crush and grind" ceramic methods have been used to the production of synthetic iron- and magnesium-containing silicates;[2-4] many processes have used high-pressure conditions to avoid the segregation of iron oxides and silica.[5,6] The "gel process", which consists of mixing alcoholic solutions of metal salts (e.g., nitrates) with silica (e.g., colloidal Ludox or hydrolyzable tetraethyl orthosilicate, TEOS) and then allowing the mixture to gel, has been used for the preparation of various synthetic silicate minerals,[7,8] including synthetic oxides of the type MgO, SiO_2, and Fe_2O_3; in the last-named case, however, evidence for the phase(s) produced was not given.[5] Recently, the preparation of olivine from silica (Nyacol), magnesium nitrate, and iron sulfate was described, but the low melting point of magnesium nitrate greatly complicated an attempt to spray-dry the precursor mixture.[6]

Thus, a new approach to the synthesis of olivine was needed, one that would enable formation of powders or gels directly from reaction mixtures while avoiding the use of metal salts that would either precipitate during reaction or complicate the drying step. This paper describes the preparation of olivine ($(Mg_{0.9}Fe_{0.1})_2SiO_4$, Fo_{90}), from metal alkoxides and an iron carbonyl. Although transition-metal carbonyl compounds have been used for the preparation of metal silicides,[9] we know of no report of such organometallics being used to prepare metal silicates. Without iron present, this new process also served as a low-temperature route to forsterite (Mg_2SiO_4, Fo_{100}), the end member of the olivine series. Forsterite has been prepared by firing mixtures of the component oxides, by coprecip-

* To whom correspondence should be addressed at the Department of Chemistry.
† Current address: Lawrence Livermore National Laboratory, P.O. Box 808, Livermore, CA 94850.
‡ Current address: American Superconductor Corp., 149 Grove Street, Watertown, MA 02172.
§ Current address: Department of Geology and Geophysics, University of Minnesota, Minneapolis, MN 55455.

(1) Ringwood, A. E. *Composition and Petrology of the Earth's Mantle*; McGraw-Hill: New York, 1975; p 618.
(2) Cooper, R. F.; Kohlstedt, D. L. *Tectonophysics* **1984**, *92*, 35–69.
(3) Karato, S.; Paterson, M. S.; FitzGerald, J. D. *J. Geophys. Res.* **1986**, *91*(B8), 8151–76.
(4) Schwenn, M. B.; Groetze, C. *Tectonophysics* **1978**, *48*, 41–60.
(5) Heald, E. F.; Reeher, J. R.; Herrington, D. R. *Am. Mineral.* **1969**, *54*, 317–320.
(6) Beeman, M. L. Ph.D. Thesis, Cornell University, 1989.
(7) Roy, R. *J. Am. Ceram. Soc.* **1956**, *39*, 145–146.
(8) Luth, W. C.; Ingamells, C. O. *Am. Mineral.* **1965**, *50*, 255–258.
(9) Aylett, B. H.; Scott, B. A.; Estes, R. D.; Beach, D. B. In *Silicon Chemistry*; Corey, E. R., Corey, J. Y., Gaspar, P. P., Ed.; Ellis Horwood Limited: Chichester, 1987; pp 357–364.

0897-4756/91/2803-0692$02.50/0